

## 3 MATERIALS AND METHODS

### 3.1 Materials

In the present section a physicochemical description of the materials that have been used will be given. All materials have been used as received and were of reagent grade.

#### 3.1.1 Lipid materials

The solid lipids used to prepare SLN and NLC consist of a mixture of several chemical compounds which needs to have a sufficiently high melting point, normally higher than 40°C. According to the purpose of the present investigation, well tolerated and *in vivo* biodegradable substances were selected for the preparation of the above mentioned lipid particles. The selected raw materials are of GRAS status and are well accepted for human use.

##### 3.1.1.1 Dynasan® 116

Dynasan® bases are market products from Contensio Chemicals GmbH (Witten, Germany). These products consist of lipid materials with a high content of microcrystalline triacylglycerols (approximately 90%) and monocarboxylic acids (approximately 10%). The triacylglycerols are glycerol esters of selected, even-numbered and unbranched fatty acids of natural origin, are free from antioxidants and other stabilizing agents.

Dynasan® 116 (triacylglycerol of palmitic acid) was the selected solid lipid for the production of clotrimazole-loaded SLN and NLC formulations. Its melting range is between 62°C and 64°C [258]. This lipid is hardly soluble both in *n*-hexane and ether as well in ethanol, and is practically insoluble in water. If Dynasan® 116 is rapidly cooled from the melt, glassy amorphous masses are initially formed which change on standing into crystalline modifications with volume expansion. The stable  $\beta$  modification has a very sharp melting point and is of triclinic structure. The lipid needs be stored in well-sealing containers and protected from light. Under these conditions this product has a shelf life of at least 3 years.

### **3.1.1.2 Compritol® 888 ATO**

Compritol® 888 ATO is a market product from Gattefossé GmbH (Weil am Rhein, Germany), based on glycerol esters of behenic acid (C<sub>22</sub>). It consists of glycerol tribehenate (28-32%), glycerol dibehenate (52-54%) and glycerol monobehenate (12-18%). The main fatty acid is behenic acid (> 85%) but other fatty acids (C<sub>16</sub>-C<sub>20</sub>) are also present.

Compritol® 888 ATO was the selected solid lipid for the production of ketoconazole-loaded SLN and NLC formulations. Its melting point is approximately 70°C [259]. Due to the presence of partial acylglycerols, this lipid has an amphiphilic character. Its hydrophilic-lipophilic balance (HLB) is approximately 2, having a drop point between 69°C and 74°C and a density value of 0.94 g/cm<sup>3</sup>. Compritol® 888 ATO has a peroxide value lower than 6 meq O<sub>2</sub>/kg, indicating a high chemical stability. It is soluble in chloroform, methylene chloride and xylene when heated and it is insoluble in ethanol, ethyl ether, mineral oils and water. It is used as lubricating agent for tablets and capsules, as a binding agent for direct compression and as a lipophilic matrix in sustained release formulations [260]. In dermal preparations, this lipid is used as viscosifying agent for oil phases in w/o or o/w emulsions and improves heat stability of emulsions. It has to be stored below 35°C because of the risk of caking, avoiding the contact with air, light, heat and moisture in its original packing.

### **3.1.1.3 Miglyol® 812**

Miglyol® 812 is a liquid triacylglycerol obtained from Caelo GmbH (Hilden, Germany). This lipid consists of medium chain triacylglycerols (C<sub>8</sub>-C<sub>10</sub>), having a density between 0.945 and 0.955 g/cm<sup>3</sup>. It is used as skin oil and as dissolution medium for many substances. Miglyol® 812 was the liquid lipid selected for the preparation of clotrimazole-loaded NLC formulations, due to its miscibility with glycerol tripalmitate at high temperatures and also due to the high solubility of clotrimazole in the obtained mixture.

### **3.1.1.4 α-Tocopherol**

Tocopherols are a family of natural and synthetic compounds, with D-α-tocopherol or vitamin E being the most familiar member [261]. These molecules contain two principle structural elements, the chroman head containing a phenolic alcohol, and the phytyl tail. This natural antioxidant is able to protect from auto-oxidation lipids present in the lipid phase of

foods and in the membrane of living cells [262, 263].  $\alpha$ -Tocopherol (Sigma-Aldrich, Deisenhofen, Germany) was the liquid lipid selected for the preparation of ketoconazole-loaded NLC formulations, due to its increasing use for protection of substances which are sensitive to oxidation, its miscibility with glycerol behenate at high temperatures and also due to the high solubility of ketoconazole in the obtained mixture.

### **3.1.2 Emulsifying agents**

The International Union of Pure and Applied Chemistry (IUPAC) defines the properties of an emulsifying agent as a surfactant, which is positively adsorbed at interfaces and lowers the interfacial tension [264]. When present in small amounts, it facilitates the formation of an emulsion or enhances its colloidal stability by decreasing either or both of the rates of coalescence or aggregation. These properties are primarily attributed to the traditional emulsifying agents. They are characterized by an amphiphilic structure and are able to form micellar aggregates. Polymers can function in the same manner, if they are sufficiently surface-active. The use of polymers as primary emulsifying agents is widely spread in food products, but they play a minor role in pharmaceutical formulations. Once SLN and NLC are stabilized by surfactants or by polymers in aqueous dispersions, in the present work the emulsifying agents used either in cosmetic products or in pharmaceutical products have been selected.

#### **3.1.2.1 Tyloxapol<sup>®</sup>**

Tyloxapol<sup>®</sup> is a polymer of 4-(1,1,3,3-tetramethylbutyl)-phenol with ethylene oxide and formaldehyde obtained from Sigma-Aldrich (Deisenhofen, Germany). It is described as a non-ionic surfactant which can be used to stabilize either o/w or w/o emulsions, having a HLB value of 12.5 and a MW of 280.40 [265, 266]. It is used as pharmaceutical excipient, mucolytic agent and surfactant for parenteral suspensions [267]. Tyloxapol<sup>®</sup> has been selected as surfactant in Dynasan<sup>®</sup> 116-based formulations.

#### **3.1.2.2 Lutrol<sup>®</sup> F68**

Lutrol<sup>®</sup> F68 or poloxamer 188 is a non-ionic surfactant obtained from BASF AG (Ludwigshafen, Germany). It consists of polyoxyethylene-polyoxypropylene block copolymer

used primarily in pharmaceutical formulations as emulsifying or solubilizing agent. The polyoxyethylene segments are hydrophilic while the polyoxypropylene segments are hydrophobic. It is freely soluble in water and alcohol, it has a HLB value of 29 [118] and a MW of 8350 [268]. Lutrol<sup>®</sup>F68 has been selected as surfactant in Compritol<sup>®</sup>888 ATO-based formulations.

### 3.1.2.3 Sodium deoxycholate

Sodium deoxycholate is a bile salt obtained from Fulka (Buchs, Switzerland). It is described as an anionic surfactant with a MW of 432, having a HLB value of 26 [269]. It has been selected as co-surfactant in Compritol<sup>®</sup>888 ATO-based formulations.

### 3.1.3 Gel forming agent

Hydrogels are semi-solid systems consisting of highly swollen, hydrophilic polymer networks that can absorb large amounts of water and drastically increase in volume. It is well known that physicochemical properties of the hydrogel depend not only on the molecular structure, the gel structure and the degree of cross-linking, but also on the content and state of water in its network.

In the present work, Carbopol<sup>®</sup>934 (polyacrylate) was obtained from BF Goodrich (Ohio, USA) and it has been used to prepare hydrogels for further entrapment of clotrimazole-loaded SLN and NLC in an optimized drug concentration. It is a carbomer polymer, with exceptional jelling abilities, mainly used in liquid and semi-solid pharmaceuticals as a suspending or viscosifying agent. It is a synthetic polymer composed of 62.6% of carboxylic groups with a high MW (approximately  $3 \times 10^6$ ) [270], formed by repeating units of acrylic acid, cross-linked with either allylsucrose or allylethers of pentaerythritol. Fig. 3.1 shows the structural formula of the carbomer polymer, i.e. acrylic acid monomer unit.

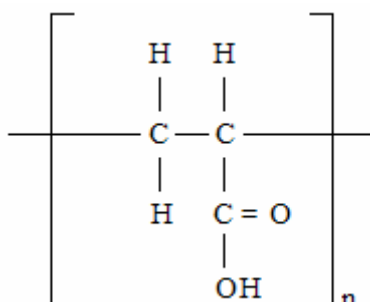


**Fig. 3.1: Acrylic acid monomer unit.**

Carbopol<sup>®</sup>934 contains between 56% and 68% of carboxylic acid (-COOH) groups as calculated on the dry basis. It forms a gel-like structure in water, alcohol and glycerol when neutralized by strong bases such as sodium hydroxide, by amines (e.g. triethanolamine) or by weak inorganic bases (e.g. ammonium hydroxide), thereby increasing the consistency and decreasing the turbidity [218]. Carbopol<sup>®</sup>934 thickens over the pH range from 5.5 to 11. Carbopols are considered to be non-toxic and non-sensitizers and do not affect the biological activities of drugs, being a major component of drug delivery systems for buccal, transdermal, ocular, rectal and nasal applications [271].

### 3.1.4 Antifungal agents

Two different imidazole antifungal agents have been selected as model drugs for the present work. According to their mechanism of action, these drugs are classified as oxidoreductases inhibitors, more specifically of lanosterol demethylase [272].

#### 3.1.4.1 Clotrimazole

Clotrimazole, or (1-2-chlorophenyl-diphenylmethyl)-1-4-imidazole, was obtained from Caelo GmbH (Hilden, Germany). It is synthesized by the reaction of o-chlorotriptylchloride with imidazole in the presence of a tertiary amine [273].

This drug is a synthetic derivative of imidazole with a broad spectrum antifungal agent that inhibits the growth of pathogenic dermatophytes [274], yeasts [275] and *Pityrosporon obiculare* (*Malassezia furfur*) [273]. Fig. 3.2 depicts the molecular structure of clotrimazole.

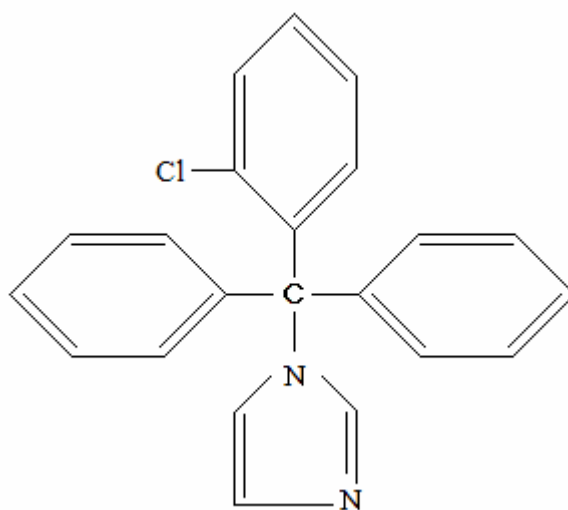


Fig. 3.2: Molecular structure of clotrimazole (MW = 344.84).

Clotrimazole is a colorless, odourless, tasteless and crystalline solid [273]. It is practically insoluble in water (< 0.01 mg/ml), soluble in chloroform and methanol (> 100 mg/ml), in ethanol (95 mg/ml) and in diethyl ether (14 mg/ml). It is freely soluble in acetone and methyl alcohol [276]. This drug is a weak base having a pKa value of 4.7 [277].

Clotrimazole is stable in the solid state under normal storage conditions [273]. It is unaffected by heat and by exposure to daylight for up to two weeks. In solution, the stability of clotrimazole is pH dependent. It is stable in alkaline media, but it decomposes into o-chlorophenyl-diphenylmethanol and imidazole in acid media [273]. A relative hydrolytic stability in solution in ethanol-water and isopropanol-water mixtures under acidic, neutral and alkaline conditions has been reported [273].

### 3.1.4.2 Ketoconazole

Ketoconazole or *cis*-1-acetyl-4-[4-[[2-(2,4-dichlorophenyl)-2-(1*H*-imidazol-1-ylmethyl)-1,3-dioxalan-4-yl]methoxy]phenyl] piperazine has been received as a generous gift of Chemo Iberica S.A. (Madrid, Spain). It is an imidazole antifungal agent, which is clinically administered both in oral and topical formulations. Due to its high permeability but low aqueous solubility, this drug is classified as a Class II active substance, since its dissolution properties in gastro-intestinal tract is insufficient under normal conditions [278]. Concerning topical formulations, this drug is considered as the standard treatment for seborrheic dermatitis [279], being the active ingredient of Nizoral<sup>®</sup> cream, as well as of an anti-dandruff shampoo [280], widely used for the treatment of human mycotic infections [281]. Fig. 3.3 depicts the molecular structure of ketoconazole.

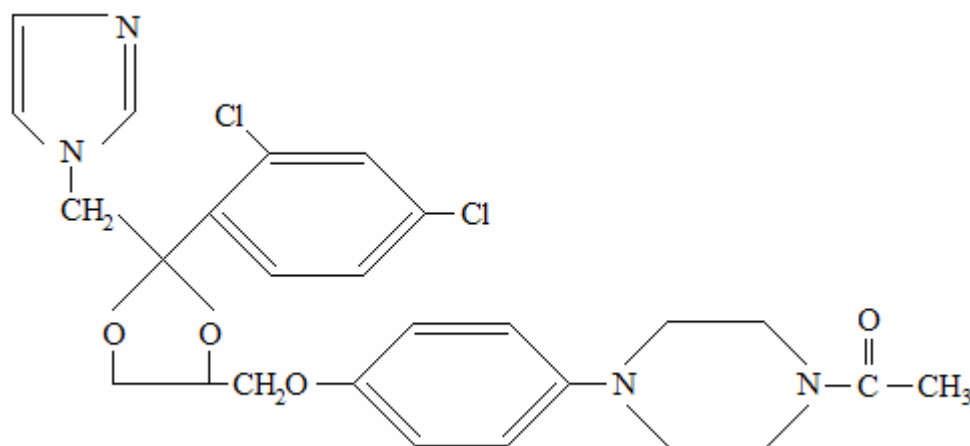


Fig. 3.3: Molecular structure of ketoconazole (MW = 531.40).

Ketoconazole is a weak base with high lipophilic properties, having a log P of 3.84 [282]. The pKa values are 2.94 and 6.51 (imidazole ring) [283]. It is a white to off white crystalline powder, which is insoluble in water, slightly soluble in warm ethanol (20 mg/ml) and warm dimethylsulfoxide (20 mg/ml), and it is freely soluble in acetone, methyl alcohol and acids. This drug is stable in the solid state under normal storage conditions. It is affected by heat and by exposure to daylight.

### 3.1.5 Other materials

#### 3.1.5.1 Commercial creams

Two different clotrimazole containing commercial formulations intended for topical use have been purchased, i.e. Fungizid-ratiopharm<sup>®</sup> cream (batch number C26808) labelled to contain 10 mg/g of clotrimazole and Canesten<sup>®</sup> cream (batch number CCTGT3) labelled to contain 10 mg/g of clotrimazole (Bayer, Germany).

A hydrophilic cream, i.e. *unguentum emulsificans aquosum* (batch number 0000095141) was purchased from a pharmacy shop (*Apotheke im Kaufzentrum*, Siemensdamm, Berlin).

#### 3.1.5.2 Glycerol

Glycerol is a distinctly hygroscopic substance, i.e. it withdrew water from the skin, especially when present in high concentrations in gels [284, 285]. It is an osmotic agent with lubricating and moisturising properties and has a wide range of pharmaceutical applications. It is miscible with water and alcohol, slightly soluble in acetone, practically insoluble in chloroform, ether and in fixed and essential oils [286].

Glycerol 85% Sigma-Aldrich (Deisenhofen, Germany) is an aqueous solution containing not less than 83.5% (m/m) and not more than 88.5% (m/m) of propane-1,2,3-triol. In the present work, this substance has been used as stabilizer, humectant and emollient in the preparation of the carbomer hydrogel.

#### 3.1.5.3 Trizma<sup>®</sup> pre-set crystals

Trizma<sup>®</sup> pre-set crystals (tris(hydroxyl-methyl) aminomethane) pH 7.0 at 25°C with a MW of 154.8, was obtained from Sigma-Aldrich (Deisenhofen, Germany). This strong amine base

has been used as neutralizing agent to adjust the pH to 6.5 for the production of the carbomer hydrogels.

#### **3.1.5.4 Methyl paraben**

Methyl paraben was obtained from Sigma-Aldrich (Deisenhofen, Germany). It is a water soluble compound that has been used as antimicrobial preservative in carbomer hydrogels. Chemically, it is a methyl ester of *p*-hydroxybenzoic acid [287]. It is a stable, non-volatile compound used as an antimicrobial preservative in foods, drugs and cosmetics for over 50 years. Methyl paraben is readily and completely absorbed through the skin.

#### **3.1.5.5 Water**

The water used in all experiments was purified water (Ph. Eur., 4<sup>th</sup> ed.) obtained from a MilliQ Plus, Millipore system (Schwalbach, Germany). It is mainly characterized by an electrical resistivity of 18 MΩ [288], and by a total organic content equal or lower than 10 ppb [289].

## **3.2 Methods**

### **3.2.1 Preparation of aqueous SLN and NLC dispersions**

The preparation of SLN and NLC was performed by the hot HPH technique, as described by Müller and Lucks [10]. The theoretical background of the HPH can be defined as schematically illustrated in Fig. 3.4. The high-pressure homogenizer consists of a high-pressure plunger pump with a subsequent relief valve [290]. The function of the plunger pump is to provide the energy level required for the relief. The relief valve (i.e. the homogenizing valve) consists of a valve seat, which is fixed, and an adjustable valve. Both parts form an adjustable radial precision gap. The gap conditions, the resistance and thus the homogenizing pressure, vary as a function of the force acting on the valve. An external impact ring forms a defined outlet cross section and prevents the valve casing from damage due to the flow.



In order to prepare SLN and NLC, the lipid phase has been melted at 5-10°C above the melting point of the solid lipid. At the same time, an aqueous surfactant solution has been prepared and heated at the same temperature. The hot lipid phase was then dispersed in the hot surfactant solution using an Ultra-Turrax T25 (Janke & Kunkel GmbH and Co KG, Staufen, Germany) at 8000 rpm for 1 min. The obtained pre-emulsion was homogenized at a temperature 5°C to 10°C higher than the melting point of the bulk lipid, using an APV Micron Lab 40 (APV Homogenizers, Unna, Germany) and applying a pressure of 500 bar and three homogenization cycles. The obtained product was filled in siliconized glass vials, which were immediately sealed. A thermostated water bath adjusted to 25°C has been used as cooling system to control the rate of cooling of the obtained product, because this is an important parameter that might influence the final thermodynamic state of the nanoparticles, i.e. the polymorphic behaviour of the solid lipid matrix.

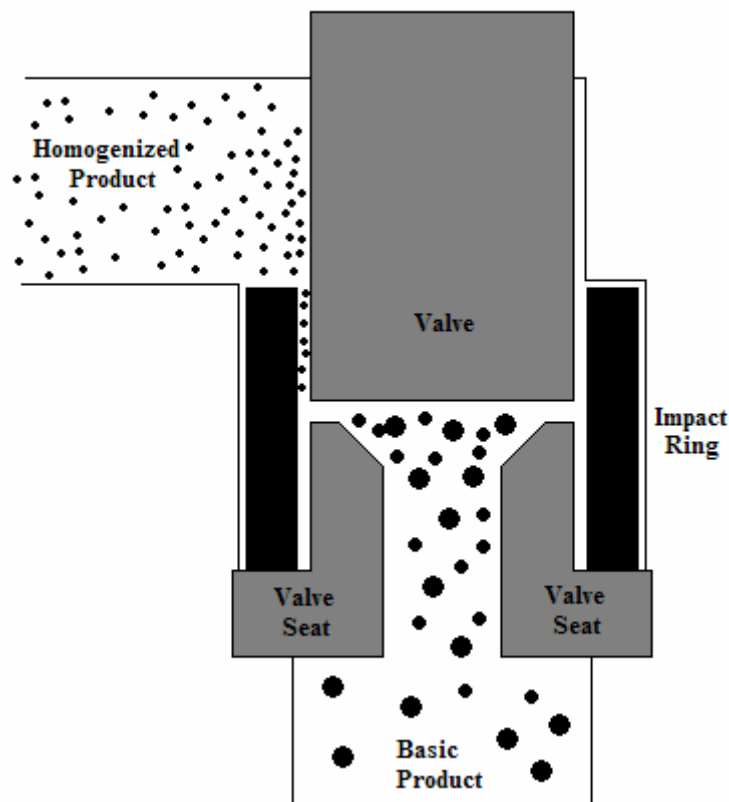


**Fig. 3.4: Schematic illustration of HPH (modified after Jahnke [290]).**

### **3.2.2 Preparation of SLN- and NLC-based semi-solid formulations**

For the preparation of SLN- and NLC-based semi-solid formulations the literature describes three main production procedures [16]:

1. built-in to o/w lotions or creams
2. blend with an existing product
3. one-step production procedure

The first procedure consists of the replacement of a part of the water in the mixture by highly concentrated lipid dispersion, followed by the production of the lotion or cream as usual. By blend with an existing product, the lotion or cream is produced as usual, if necessary reducing the water content, followed by the blend of the product with highly concentrated lipid dispersion.

These two approaches exploit the benefits of an already established product and combine them with the additional advantages of lipid particles having a solid matrix, such as the protection of chemically labile compounds or occlusion effect and, therefore, hydration.

When suggesting the first procedure, one can ask in which extent the lipid nanoparticles are physically stable during the production process of the lotion or cream [16]. When having an optimized formulation, lipid nanoparticles are sufficiently stabilized to avoid coalescence with each other or coalescence with oil droplets of the inner phase of the lotion or cream. Depending on the production temperature of the cream and the melting point of the lipid matrix of the nanoparticles, they might melt during the production process of the cream but at the end of this process they recrystallize during cooling of the product.

When admixing lipid nanoparticles loaded with active compounds to an existing product (second approach), problems with the loading capacity might occur. This is especially valid when mixing relatively low concentrated lipid nanoparticle dispersions. Only a certain percentage of the dispersion can be admixed. This aqueous lipid nanoparticle dispersion contains only a certain percentage of lipid mass, the lipid mass contains only a certain percentage of active compounds. This is less problematic when mixing highly concentrated lipid nanoparticle dispersions.

By one-step production procedure the lipid phase of the final product consists of 100% of lipid nanoparticles. If necessary, addition of a viscosity enhancer can be performed to increase the consistency of the final product.

In the present work, the second approach has been selected for the preparation of hydrogels containing SLN and NLC. The final formulations were composed of 5% glycerol, 50% aqueous SLN or NLC dispersion, a sufficient amount of the gel-forming polymer and purified water. To prepare clear, uniform air-free carbomer hydrogels certain processing conditions have been provided. In order to obtain a uniform smooth dispersion, the gel-forming polymer, glycerol and water were weighed in a beaker and stirred with a high speed stirrer (Cito Unguator Konieczko, Bamberg, Germany) at approximately 1000 rpm for 5 min. This initial high-shear mixing was followed by low-shear planetary mixing during the neutralization jelling process performed by addition of Trizma<sup>®</sup>Pre-set crystals pH 7.0 until reaching the pH of 6.5. Methyl paraben was used as preservative of the semi-solid systems and, therefore, it has been added to the water phase during the preparation of the hydrogels. Finally, the aqueous SLN or NLC dispersion was added to the freshly prepared hydrogels under continuous stirring at 1000 rpm for 3 min.

### **3.2.3 Measurement of particle size and zeta potential**

#### **3.2.3.1 Laser diffractometry**

Laser light diffraction (LD) is a technique used for the determination of the sizes of particles in the range of 0.5  $\mu\text{m}$  to 100  $\mu\text{m}$ . The laser diffractometer consists of a laser beam, which is expanded and passes through the measuring cell (Fig. 3.5). In order to calculate the size distribution, the instrument uses Fraunhofer diffraction of laser scattered from particles in dispersion. The laser light is diffracted by the particle surface and leads to the formation of a Fraunhofer diffraction pattern on the multielement detector placed behind the cell. These particles cause diffraction of laser light through different angles and create a diffraction pattern of light rings with varying radii. The detector consists of 32 concentric rings plotting the intensity on each ring versus the ring number yields the Fraunhofer diffraction pattern.

The diffraction patterns created by differently sized particles are detected on a ring detector and are used to calculate the size distribution. The diffraction pattern depends on the particle size, i.e. small particles create a large diffraction angle, while large particles create a small diffraction angle. This leads to the highest light intensity on the inner rings in case of large particles (low ring number), and on the outer rings in case of small particles (high ring number).

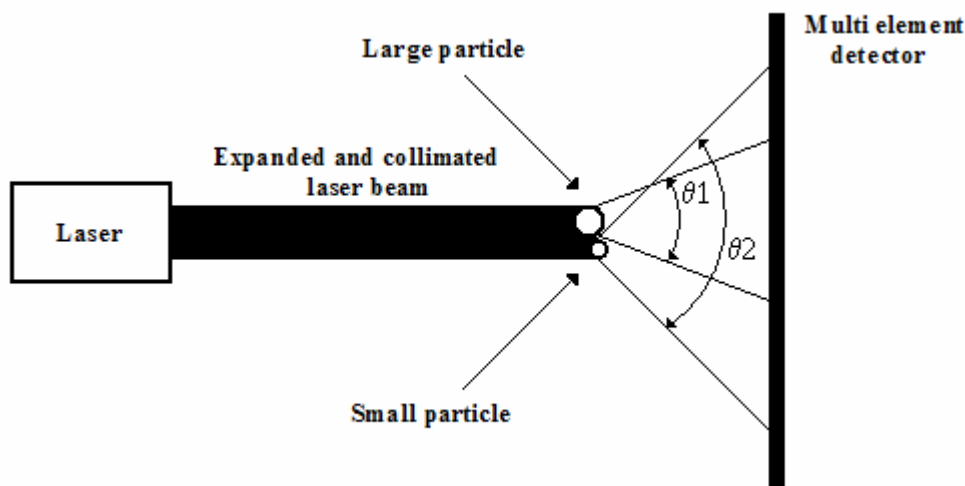


**Fig. 3.5: Principle of operation of a laser diffractometer. The diffraction angles and the diffraction pattern created are a characteristic function of particle size. The diffraction angle is small for large particles and large for small particles (modified after Müller [291]).**

The laser diffractometers are composed of a laser, an optical unit to expand the beam, and a Fourier Transform lens for focussing the scattered light onto a ring detector (Fig. 3.6).

The particle dispersion is located in a measuring cell at a certain distance from the receiver lens. The patterns of particles located in different areas of the cells (moving particles) are projected on identical rings by the use of a Fourier transform lens. The intensity of the patterns increases with the number of diffracting particles. This allows the calculation of the particle concentration from the intensity. The simultaneous presence of particles with different sizes leads to diffraction patterns, which are the superposition of the patterns specific for each size. This pattern can be mathematically resolved to yield a volume distribution of the particles. The volume distribution can be calculated applying the Fraunhofer theory. However, this theory becomes in error for particles having a size lower than  $4 \mu\text{m}$  and particles dispersed in liquids instead of gases. In samples dispersed in liquids and/or contained particle fractions below  $4 \mu\text{m}$ , a calculation should be performed using the Mie theory being generally valid for all particles. However, in contrast to the Fraunhofer theory using the Mie theory requires the knowledge of diffraction index and absorption of the sample.

A practical advantage of the laser diffractometers is the fact that any transparent dispersion medium can be used, such as aqueous or organic liquids and air. Size measurements can also be performed maintaining the particles in their original dispersion medium, thereby minimizing changes in the sample due to modifications in the measurement conditions.

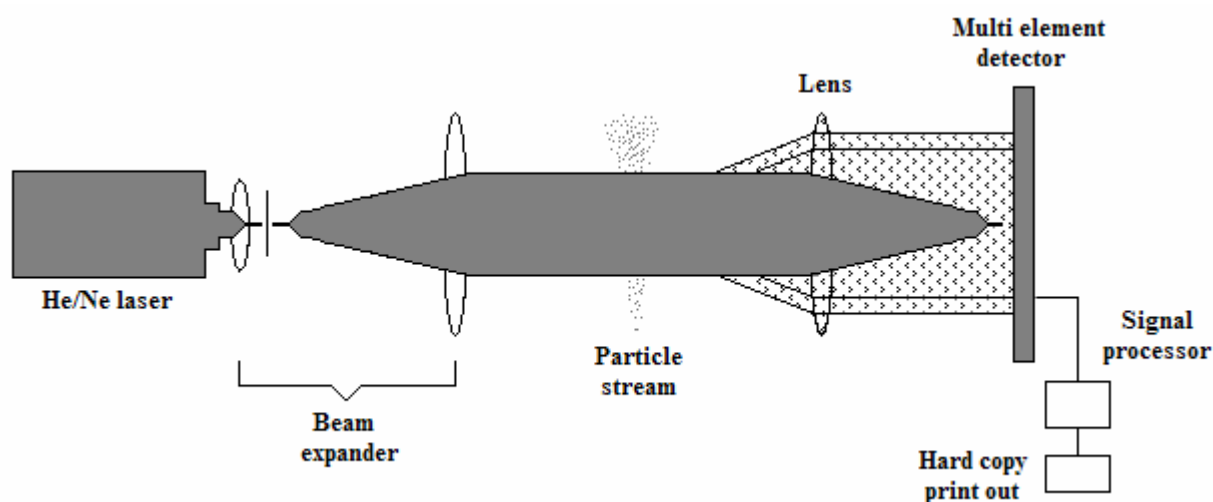


**Fig. 3.6: Schematic representation of a laser diffractometer (modified after Müller [291]).**

As the light enters the particle, it can be absorbed or refracted. Generally, a combination of both of these processes occurs. These effects are quantified by the relative refractive index of the material. For most common organic materials, this index is a well defined quantity which can be obtained from reference texts. However, the situation is more complex with absorbing or reflective materials. To allow the absorption and reflection, it is necessary to define the refractive index as a complex quantity, which means a quantity having a real and an imaginary part. The simplest interpretation of the complex refractive index is that the real part describes the material refractive properties, while the imaginary part describes its light absorbing properties. The refractive index of a completely transparent material would consist of only a real part, and the imaginary part would be zero. Alternatively, a coloured material would have a refractive index with both a real part (describing its refractive properties) and an imaginary part (describing its absorbing properties). Both of these quantities influence the light scattering, and for many materials which cannot be prepared in large crystals, light scattering from particulates provides the only way of investigating their optical properties. Unfortunately, data on the complex refractive index of many systems is difficult to find in the literature, since it has only been investigated in detail for a small number of well characterized materials [292]. Concerning lipid nanoparticles the real part is 1.456 and the imaginary part is 0.01.

For the assessment of the particle size the instrument applies the Mie theory. The theory is derived by solving the Maxwell's equations for the incidence of a plane wave front on a particle. It calculates the induced electric field patterns in the particles (the so-called spherical harmonic electric field modes), then calculates the diffraction pattern from the light radiated

by these modes. In order to calculate the light scattering pattern, it is only necessary to specify the complex refractive index of the sample material, the refractive index of the suspending medium, the particle size, and the wavelength of light being scattered. These are then combined into two dimensionless parameters, which are the relative refractive index  $N$ , and the size parameter  $x$ . The size parameter is then given by:

$$x = \frac{2\pi N a}{\lambda} \quad (3)$$

where  $a$  is the particle radius and  $\lambda$  the wavelength of light. The size parameter thus describes the particle size in terms of the wavelength of scattered light, i.e. the scattering pattern is dependent only on the size parameter and not on the actual particle size.

In the present work, LD was performed using a Coulter<sup>®</sup>LS 230 (Beckmann-Coulter Electronics, Germany). LD data were evaluated using volume distribution, which means that a diameter 90% (LD90) value of 1  $\mu\text{m}$  indicates that 90% of the particles possess a diameter of 1  $\mu\text{m}$  or less.

In the case of SLN- and NLC-based semi-solid formulations, prior to particle size analysis by LD, the formulations have been diluted with double-distilled water to weak opalescence.

### **3.2.3.2 Photon correlation spectroscopy**

Photon correlation spectroscopy (PCS) is a technique employed to determine the mean particle size (PCS diameter) and size distribution (polydispersity index, PI) [291]. It is a light-scattering experiment in which the statistical intensity fluctuations in light scattered from the particles are measured. These fluctuations are due to the random Brownian motion of the particles.

PCS device consists of a laser light scattering technique suitable for application to particles ranging in size from 5 nm to approximately 3  $\mu\text{m}$ . A focused laser beam illuminates a small volume of the sample, which consists of a dilute suspension of particles. The light scattered from these particles is collected by a lens and its intensity is measured by a photomultiplier. If the sample was completely uniform, a constant light intensity would be scattered. Since the diffusion rate, or velocity, of the particles is determined by their size (given that fluid viscosity and temperature are known or constant), information about the size is contained in the rate of fluctuation of scattered light intensity. The lower particle size limit for measurement is determined by the scattering intensity and the experimental noise. If the suspended particles are small, they diffuse relatively fast, and so the fluctuations in the

scattered light are correspondingly rapid. Alternatively, if the particles are large, their movement is slower, and the scattered light fluctuations occur over a longer time scale. Consequently, it will be appreciated that the temporal variations in scattered light intensity contain information which could allow the diffusion coefficient of the particles to be obtained. Once the diffusion coefficient is known, the equivalent diffusional spherical diameter can be obtained applying the Stokes-Einstein equation, which relates the diffusion coefficient  $D$  of a spherical particle to its diameter  $d$ :

$$d = \frac{kT}{3\pi\rho D} \quad (4)$$

where  $\rho$  is the viscosity of the surrounding medium,  $k$  is the Boltzmann's constant,  $T$  is the absolute temperature. The problem is thus the extraction of the diffusion coefficient from the noise signal in the scattered light intensity. Since the frequency of the noise depends on the diffusion coefficient, it could be suggested that the noise frequency spectrum in the photomultiplier signal can be measured with a spectrum analyser. The frequency spectrum  $P(\omega)$  of the intensity noise scattered from a collection of randomly diffusing monodisperse spheres can be shown to have a Lorentzian distribution:

$$P(\omega) = \frac{2DK^2/\omega}{\omega^2 + (2DK^2)^2} \quad (5)$$

where  $\omega$  is the frequency,  $D$  the diffusion coefficient and  $K$  scattering vector, which is given by:

$$K = \frac{4\pi n}{\lambda} \sin \frac{\theta}{2} \quad (6)$$

where  $n$  is the refractive index of the suspension medium,  $\lambda$  is the wavelength of the light and  $\theta$  is the scattering angle.

In practice, this measurement is not normally performed using frequency analysis techniques, but by measurement in the time domain, since this is accomplished using less complex equipment and leads to a more straightforward analysis. The time domain equivalent of the frequency spectrum is called the intensity auto-correlation function  $G(\tau)$ , and it is obtained by taking the Fourier transform of the (frequency domain) noise spectrum. The auto-correlation function of a fluctuating quantity measured as a function of time,  $I(t)$  (e.g. a scattered light intensity), which has been measured from time  $t = 0$  to time  $t = T$ , is defined formally as follows:

$$G(\tau) = 1 + e^{-2DK^2\tau} \quad (7)$$

where  $D$  is the diffusion coefficient of particles,  $K$  is the scattering vector of light and  $\tau$  is the sample time.

The schematic set up of a PCS device is illustrated in Fig. 3.7. The apparatus consists of a laser, a temperature controlled sample cell and a photomultiplier for the detection of the scattered light at a certain angle (e.g.  $90^\circ$ ) [291]. The photomultiplier signal is transferred to a correlator for calculation of the  $G(\tau)$ . This  $G(\tau)$  is relayed to a microprocessor for calculation of  $D$  and the correlated mean particle size.

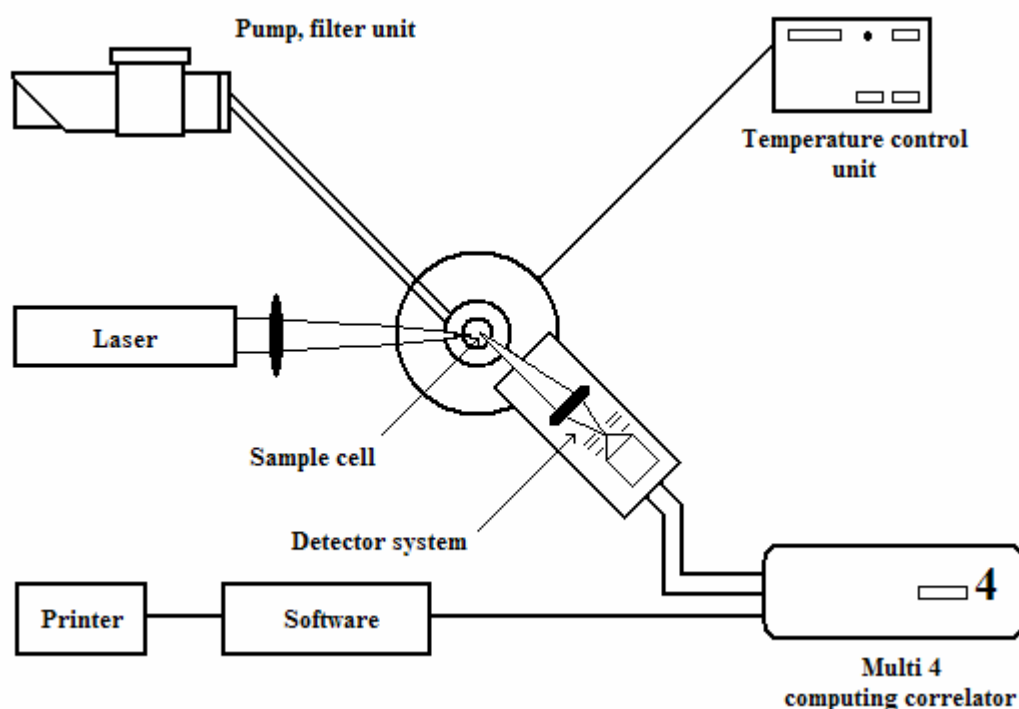


**Fig. 3.7: Schematic representation of the PCS device (modified after Müller [291]).**

PCS does not exploit the absolute intensity of the scattered light, but rather fluctuations in intensity. Small particles diffuse faster than large ones causing a stronger fluctuation in the scattering signal and a more rapid decaying  $G(\tau)$ . For a monodisperse particle population  $G(\tau)$  is a single exponential, but in the presence of more than one size the function is polyexponential.

Deviation from a single exponential is used to calculate the PI, which is a measure of the width of the size distribution. An ideal, monodisperse formulation has a PI of zero.

PCS diameter gives information about the average particle size. The measured PCS diameter is based on the intensity of scattered light and therefore is not identical to the numeric diameter except in case of monodisperse particle suspensions. For polydisperse samples, PCS



diameter is larger because it is based on the scattering intensity of the particles. The scattering intensity does not linearly depend on the particle size, but it is proportionally related to the 6<sup>th</sup> power of the radius (Rayleigh scattering,  $\Gamma r^6/\lambda^4$ ). Therefore, the broader the particle size distribution, the greater is the disparity between the PCS and number diameters. This phenomenon makes the measurements of PCS very sensitive for following aggregation or de-aggregation processes in suspensions.

In the present work, for PCS measurements all samples have been diluted with double-distilled water to suitable concentration and measured by a Malvern Zetasizer IV apparatus (Malvern Instruments, UK). In the case of SLN- and NLC-based semi-solid formulations, prior to particle size analysis by PCS, the formulations have been diluted with double-distilled water to weak opalescence.

### 3.2.3.3 Zeta potential and electrophoretic mobility

Although it is not a description of particle size, measurement of zeta potential has become inextricably connected with the study and characterization of colloidal dispersions, and since it is also performed by optical correlation techniques, a brief description may be valuable once it is also a parameter highly useful for the assessment of the physical stability of colloidal dispersions.

Surfaces of particles in suspension develop a charge due to adsorption of ions or ionization of surface groups, and the charge is correspondingly dependent on both the surface chemistry and the environment of the particles (Fig. 3.8). The surface charge generates a potential around the particle, which is high near the surface and decays with distance into the suspending medium. If the particle is placed in an electric field, it will drift with a characteristic velocity  $u$ . The velocity per unit field strength is called the electrophoretic mobility, and it is normally expressed in micrometers per second per volt per centimetre ( $\mu\text{m/s}/(\text{V/cm})$ ). As the particle moves it carries with it an ionic environment which extends a small distance into the solvent. The spherical surface separating the moving particle, ions and solvent from the stationary surroundings is called the surface of hydrodynamic shear, the electrophoretic mobility is determined by the potential at this surface, which is termed the zeta potential  $\zeta$ . The zeta potential can be determined from the electrophoretic mobility using the Smoluchowski equation, which is applied to large particles in weak electrolytes:

$$u = \frac{\epsilon \zeta}{\eta} \quad (8)$$

where  $\eta$  is viscosity of the dispersion medium and  $\epsilon$  the permittivity of the environment, i.e. dielectric constant. Particle velocity  $v$  can be then expressed in relation to the electrical field strength  $E$  as electrophoretic mobility  $\mu$  using the following equation:

$$\mu = \frac{v}{E} \quad (9)$$

The electrophoretic mobility  $\mu$  can be converted to  $\zeta$  using the Helmholtz equation:

$$\zeta = \frac{4v\pi\eta}{E\epsilon} \quad (10)$$

In weak electrolytes the potential does not change rapidly with distance into the solvent, and so zeta potential is often equated with the potential on the colloid surface, or the Stern potential, and therefore it is used to characterize the surface chemistry of the particles.

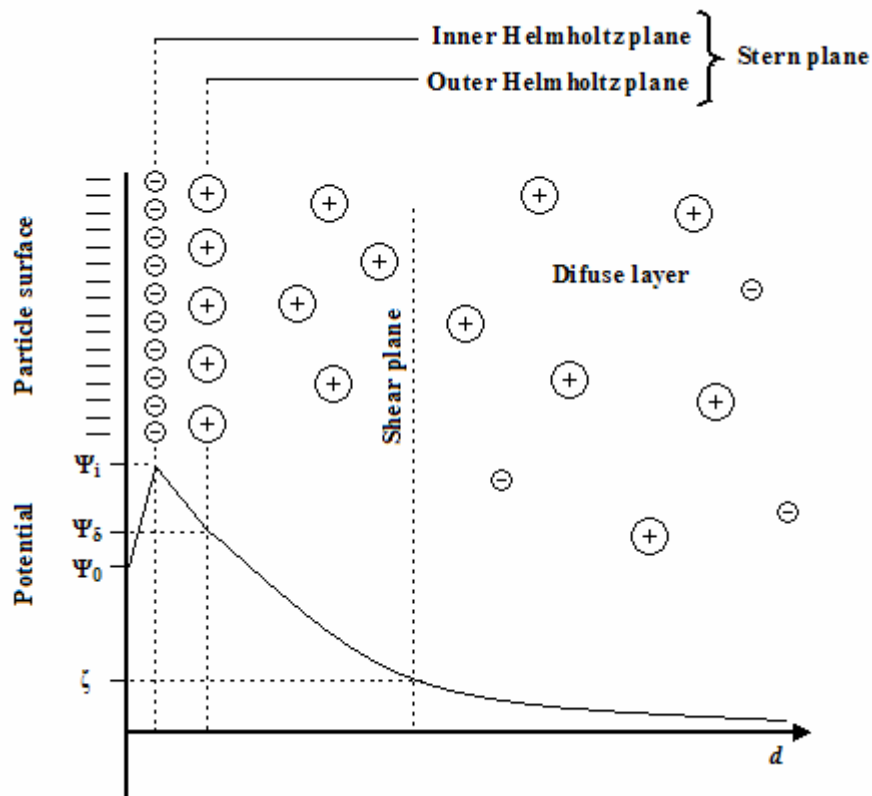


**Fig. 3.8: Schematic representation of different surface potentials associated to the particle in aqueous medium. Formation of Stern plane and diffuse layer on particle surface.  $\Psi_0$ , Nernst potential;  $\Psi_i$ , potential of inner Helmholtz plane,  $\Psi_\delta$ , Stern potential;  $\delta$ , thickness of Stern plane;  $\zeta$ , zeta potential at the surface of shear;  $d$ , distance from the particle surface (modified after Müller [291]).**

The adsorbed monolayer of ions at the particle surface consists of fixed, dehydrated and in most cases negatively charged ions (inner Helmholtz layer). These negative ions increase the surface potential (Nernst potential,  $\Psi_0$ ) to the potential of the inner Helmholtz layer,  $\Psi_i$ . The next monolayer (outer Helmholtz plane) consists of fixed but hydrated positive ions reducing the potential to the potential of the Stern plane ( $\Psi_\delta$ ) where  $\delta$  is the thickness of the Stern plane. In the diffuse layer the potential drops towards zero. During the movement of the particle a part of the diffuse layer will be stripped to reveal a potential at the shear plane. This potential is called zeta potential ( $\zeta$  or ZP) and it is an indirect measurement of the surface charge because its magnitude depends on the Nernst potential.

The zeta potential can be measured by determination of the movement velocity of the particles in an electric field (electrophoresis measurements). Conventional instruments use a light microscope to observe the particle movement, whilst the modern zetameters use laser Doppler anemometry (LDA) to determine the particle velocity.

A LDA set up consists of a laser, a beam splitter and a lens which focuses the beams into the measuring volume, forming a beam crossover. Particles move through the beam crossover and scatter laser light. The scattered light is detected in the forward direction and projected by collecting optics onto a photomultiplier. The frequency of the laser light scattered by the particles differs from the frequency of the incident beam. This frequency shift is caused by the Doppler effect and it is a function of the particle velocity. As mentioned before, the Malvern Zetasizer IV apparatus uses the photomultiplier signal to calculate a “G( $\tau$ )”, which is transferred via Fourier Transform to the frequency spectrum of the scattered light.

In the present work, for the zeta potential measurements a Malvern Zetasizer IV apparatus (Malvern Instruments, UK) has been used. Formulations have been previously diluted with double-distilled water adjusted to a conductivity 50  $\mu\text{S}/\text{cm}$  with a solution of 0.9% NaCl (if not otherwise stated) [293].

### **3.2.4 Imaging analysis**

All substances that are transparent when examined under a microscope that has crossed polarizing filters are either isotropic or anisotropic [294]. Amorphous substances, such as supercooled melts and non-crystalline solid organic compounds, or substances with cubic crystal lattices are isotropic materials, having a single refractive index. Materials with more than one refractive index are anisotropic and appear bright with brilliant colours (birefringence) against a black polarized background. The interference colours depend upon

the crystal thickness and the differences are either uniaxial, having two refractive indices, or biaxial, having three principal refractive indices.

Most drugs are biaxial, corresponding to either an orthorhombic, monoclinic or triclinic crystal system.

The major advantage that microscopic techniques possess over most of the afore-mentioned methods of size analysis is that the particle profile itself is measured, rather than some property which is dependent on particle size. In order to analyse lipid nanoparticles light and electron microscopy have been used.

#### **3.2.4.1 Light microscopy analysis**

The size of particles which can be imaged by microscopy is limited by the diffraction of the light used to form the image. The resolution of the microscope is given approximately as the wavelength of the light divided by the numerical aperture of the microscope objective.

Investigations have been performed using a Leitz Orthoplan Microscope (Wetzlar, Germany) at 100x, 400x and 1000x with an oil immersion objective, in order to determine the presence/absence of drug crystals in the melted lipid and in the developed formulations, as well as to determine the particle size of SLN and NLC. Polarised light was used applying a magnification of 630x to search for particles and/or drug crystals larger than 1  $\mu\text{m}$ . Oil immersion and magnification of 1000x were employed to detect nanoparticles and/or drug nanocrystals with a size of a few hundred nanometers. The detection limit of the light microscope is about 0.2  $\mu\text{m}$ . The use of polarised light enables the imaging of nanoparticles in the range between 200-300 nm, however it cannot measure the particle size accurately.

#### **3.2.4.2 Scanning electron microscopy analysis**

Scanning electron microscopy (SEM) is useful since it allows particles much smaller than 1  $\mu\text{m}$  to be measured. Aqueous dispersions of lipid nanoparticles were spread on a sample holder with double sided tape and coated under an argon atmosphere with gold to a thickness of 6.5 nm (SCD 040, Balt-Tec GmbH, Witten, Germany). The samples have been observed with a scanning electron microscope (S-4000, Hitachi High-Technologies Europe GmbH, Krefeld, Germany) using secondary electron imaging at 10 keV in order to examine the surface morphology and to assess the particle size of lipid nanoparticles. SEM studies have

been performed together with Mr. Gernert at the *Zentraleinrichtung Elektronenmikroskopie* (Technische Universität Berlin, Germany).

### **3.2.5 Thermal analysis**

#### **3.2.5.1 Thermal gravimetry analysis**

Thermal gravimetry analysis (TGA) uses a thermo-balance, which allows for ongoing monitoring of sample weight as a function of temperature [295]. This procedure involves a controlled heating or cooling programme or a maintained fixed temperature. Instrumentation is typically a balance with a data acquisition system to record the loss of weight. A furnace surrounds the sample holder and ancillary controls to modulate such as furnace temperature and operational atmosphere are available. The actual nature of the equipment can vary with the application, e.g. maximum operating temperature and sample size, but for pharmaceutical studies temperatures of up to 350°C and sample sizes of 5-20 mg are generally adequate.

TGA measurements have been performed using a Mettler TG-DTA analyser (Mettler Toledo, Gießen, Germany). The loss of weight was recorded weighting approximately 10 mg of model drug, which was heated in an aluminium oxide crucible from 25°C to 200°C and cooled again down to 25°C, at a rate of 10 K/min.

#### **3.2.5.2 Differential scanning calorimetry analysis**

Differential scanning calorimetry (DSC) is frequently used to provide information on both physical and energetic properties of a compound or formulation. DSC measures the heat loss or gain resulting from physical or chemical changes within a sample as a function of the temperature.

The instrumentation which is usually used is a heat-flux DSC system. A constantan disc provides the primary means of transferring heat to sample and reference positions, whilst also functioning as one element of the temperature-measuring thermo-electric junctions [295]. During the scan the sample and reference are contained in aluminium pans which are positioned on raised platforms on the constantan disc (thermo-electric disc). Heat is transferred through the disc and through the sample pan to the contained sample and reference. The differential heat flow is monitored by chromel-constantan area thermo-couples formed by the junction of the constantan disc and the chromel wafer. There is a chromel wafer

covering the underside of the raised platforms beneath both the sample and reference pans. The sample temperature is monitored directly via chromel-alumel thermo-couples formed from chromel and alumel wires connected to the underside of the chromel wafers. Software linearization of the cell calibration is used to maintain calorimetric sensitivity. The cell has a volume of 2 ml and can be used with various non-corrosive inert atmospheres, as well as oxidizing and reducing atmospheres. Available sample pans (hermetic, open or sealed) allow sample volumes of 0.1 ml which can be up to 100 mg depending on sample density.

Examples of heat-absorbing processes (endothermic measurements) are fusion, boiling, sublimation, vaporization, desolvation and solid-solid transitions. Crystallization is usually an exothermic process, i.e. energy is liberated. Qualitative measurements of these processes have many applications, such as the study of purity, polymorphism, solvation, degradation and compatibility of substances. DSC analysis has been used to characterize the state and the degree of crystallinity of lipid dispersions, semi-solid systems, polymers and liposomes. It allows the study of the melting and crystallization behaviour of crystalline material like lipid nanoparticles [296-299]. The breakdown or fusion of the crystal lattice by heating or cooling the sample gives information on polymorphism, crystal ordering, eutectic mixtures or glass transition processes. DSC experiments are useful to understand solid dispersions like solid solutions, simple eutectic mixtures or, as in the case of SLN and NLC, drug and lipid interactions and the mixing behaviour of solid lipids with liquid lipids, such as oils.

In general, a melting point depression is observed when transforming the bulk lipid to nanoparticulate form. This melting point depression is described by the Gibbs-Thomson equation which itself is derived from the Kelvin equation:

$$\ln\left(\frac{T}{T_0}\right) = -\frac{2\gamma V_s}{r \Delta H} \quad (11)$$

where  $T$  represents the melting point of the particle, and it is always smaller than the melting point of the bulk material  $T_0$ . The molar volume of the substance is characterized by  $V_s$ ,  $r$  is the radius of the particle,  $\Delta H$  is the molar melting enthalpy and  $\gamma$  is the interfacial energy at the solid-lipid interface. For characterizing crystal forms,  $\Delta H$  can be obtained from the area under the DSC curve of the melting endotherm.

An additional melting point depression occurs when a foreign compound is dissolved in the lipid matrix, such as surfactant molecules that will partition from the water phase to the lipid phase. Therefore, drug-loaded SLN will show a melting point depression in case of a molecularly dispersed drug is present.

In order to compare the crystallinity between the developed formulations a useful parameter is the recrystallization index (RI), which is defined as the percentage of the lipid matrix that has recrystallized during storage time. The RI can be calculated according to the following equation [300]:

$$\text{RI (\%)} = \frac{\Delta H_{\text{aqueous SLN or NLC dispersion}}}{\Delta H_{\text{bulk material}} \times \text{Concentration}_{\text{lipid phase}}} \times 100 \quad (12)$$

where  $\Delta H$  is the molar melting enthalpy given by J/g and the concentration is given by the percentage of lipid phase.

In the present work, DSC measurements have been performed on a Mettler DSC 821e apparatus (Mettler Toledo, Gießen, Germany). A sufficient amount of aqueous dispersion having ca. 1-2 mg of solid lipid has been accurately weighted in 40  $\mu\text{l}$  aluminium pans. DSC scans have been recorded from 25°C to 85°C at a heating rate of 5 K/min, using an empty pan as reference. Melting points correspond to the maximum of the heating curve. For the analysis of pure model drugs the heating run has been recorded from 20°C to 200°C and cooled to 20°C under liquid nitrogen at a rate of 10 K/min. Polymorphic forms have been assigned by comparison with X-ray diffraction data.

### 3.2.6 X-ray diffraction analysis

An important technique for establishing the reproducibility of a polymorphic form between different batches is X-ray diffraction, i.e. wide-angle X-ray scattering (WAXS) and small-angle X-ray scattering (SAXS). Fig. 3.9 illustrates the theory of this technique.

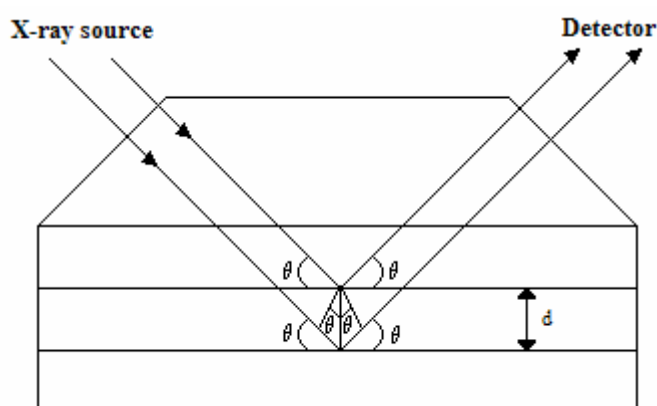


**Fig. 3.9: Schematic representation of X-ray diffraction (modified after Barber [301]).**

When a monochromatic X-ray beam is focused on a crystal, the scattered X-rays from the regularly placed atoms interfere with each other, giving strong diffraction signals in particular directions, since the interatomic distances are of the same order as the X-ray wavelength. The directions of the diffracted beams are related to the shape and dimensions of the unit cell of the crystalline lattice. The diffraction intensity depends on the disposition of the atoms within the unit cell. This technique allows amorphous and crystalline materials to be differentiated. Crystalline materials display many diffractions bands, whereas amorphous compounds present a more or less regular baseline.

The crystal diffracts X-rays similar to a diffraction grating, whose plane diffracts ordinary light. The three-dimensional crystal functions like a series of plane gratings stacked one above the other [302]. The wavelength of the X-rays  $\lambda$  is related to the angle of incidence  $\theta$  and to the interatomic distance  $d$  by Bragg's equation:

$$d = \frac{\lambda}{\sin 2\theta} \quad (13)$$

For a single crystal, the diffracted X-rays consist of a few lines. With powder, due to a random distribution of crystals, the diffraction pattern consists of a series of concentric cones with a common apex on the sample. The atoms in a crystal possess the power of diffracting the X-ray beam. Each substance scatters the beam in a particular diffraction pattern, producing a fingerprint for each atom crystal or molecule.

If an unknown powder sample is to be identified, its diffraction pattern may be compared with those of known substances or its  $d$  values calculated from the diffraction diagram and compared with the  $d$  values of known compounds.

If the diffraction pattern of a single crystal is to be determined, the crystal is mounted on a thin glass capillary and the capillary is fastened to a brass pin. A substance in powder form can be ground finely and transformed into a small rod using collodion as a binder or held in a specific device with an open cup. Samples like aqueous dispersions can be transformed into a paste, using a thickening agent, such as locust bean gum [19] and xanthan gum [160].

X-ray diffraction has been used for the study of molecular structure and polymorphism of lipid nanoparticles [19, 133, 156, 160, 164, 172, 209, 303].

In the present work, X-ray diffraction patterns were obtained using the WAXS (2 Theta = 4-40°) on a Philips PW 1830 X-ray generator (Philips, Amedo, The Netherlands) with a copper anode (Cu-K $\alpha$  radiation,  $\lambda=0.15418$  nm) using a Goniometer PW18120 as a detector. Data of the scattered radiation were detected with a blend local-sensitive detector using an anode voltage of 40 kV, a current of 25 mA and a scan rate of 0.5° per min. Prior to analysis, aqueous SLN and NLC dispersions were transformed into a paste using locust bean



gum as thickening agent, i.e. 1 ml of dispersion was mixed with approximately 1 mg of gum. For the analysis of pure drug and/or lipids the powders have been mounted on a thin glass capillary being fastened to a brass pin without any previous sample treatment.

### 3.2.7 High performance liquid chromatography analysis

High performance liquid chromatography (HPLC) analysis has been performed according to the USP XXIV using a Kroma System 2000 (Kontron Instruments, Berlin, Germany) running in the isocratic modus. The system consisted of a HPLC pump 220, an Auto-sampler T360 and a UV detector 430. A water bath Haake W90 (Haake, Karlsruhe, Germany) was used for the control of the temperature. UV detection was performed using a cartridge column Nucleosil-120 C18 (3  $\mu$ m) having a length of 100x4 mm ID (Knauer, Berlin, Germany). As test conditions a mobile phase consisting of methanol/water 8:2 (v/v) was used, with an injection volume of 1  $\mu$ l, flow rate of 1.5 ml/min, pressure of 14.8 mPa, at room temperature. For the assessment of drug recovery of model drugs appropriate calibration curves have been obtained using acetone as dissolution medium. Those curves are depicted in Figs. 3.10 and 3.11 for clotrimazole and ketoconazole, respectively. For the assay of clotrimazole, a calibration curve has been obtained from a series of standard solutions of drug in acetone, ranging from 0.005 mg/ml to 0.06 mg/ml. Concerning the ketoconazole assay, a calibration curve has also been obtained from a series of standard solutions of drug in acetone, ranging from 25  $\mu$ g/ml to 250  $\mu$ g/ml.

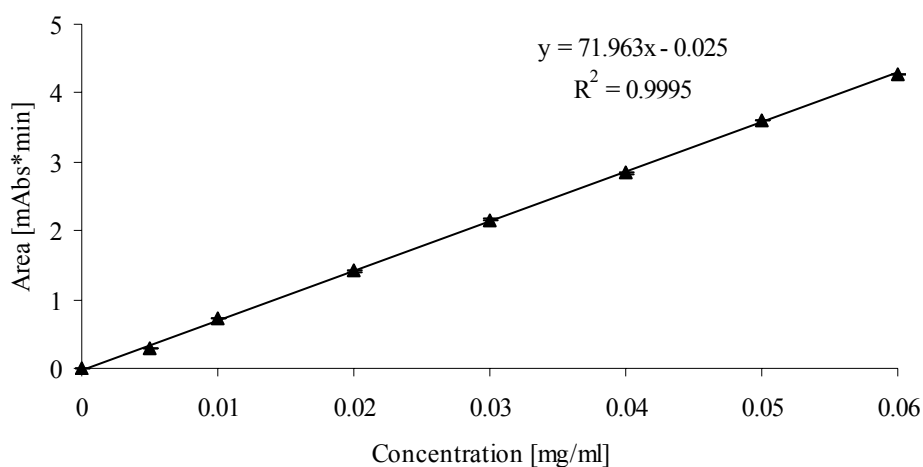


**Fig. 3.10: Calibration curve for clotrimazole in acetone.**

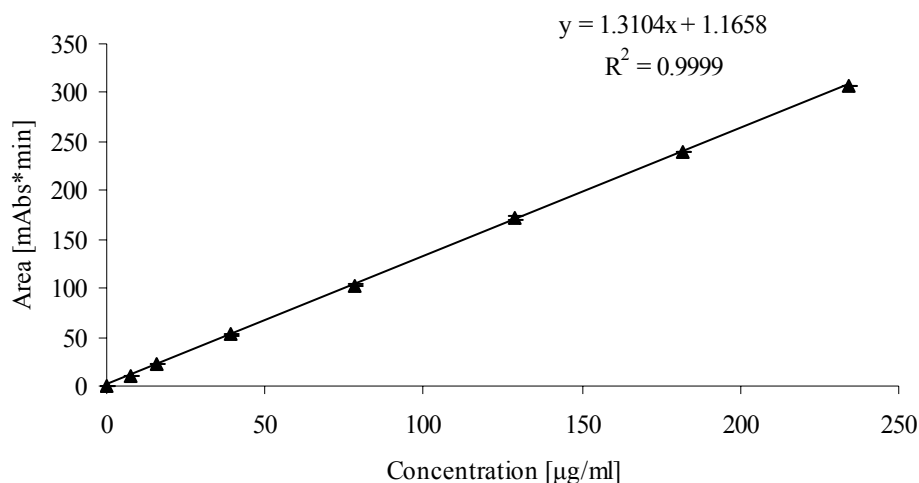


**Fig. 3.11: Calibration curve for ketoconazole in acetone.**

The Kontron HPLC software was used for the analysis of the results, i.e. integration of the peaks. The retention time for clotrimazole was 11.4 min and for ketoconazole was 9.3 min. For both drugs, the wavelength of maximum absorption was 254 nm and 220 nm, respectively. The total amount of incorporated drug in the lipid nanoparticles was determined by dissolving an appropriate amount of aqueous dispersions in acetone.

### 3.2.8 Experimental assessment of drug release from developed formulations

In matrix systems such as lipid nanoparticles the drug is incorporated in the lipid matrix either in dissolved or in dispersed form [12, 223]. Therefore, the solubility of the drug in the lipid matrix becomes a very important controlling factor of the drug release from SLN and NLC. When the initial drug loading is below the solubility limit, release is achieved by simple diffusion through the lipid. However, when the drug loading is above the solubility limit, dissolution of the drug in the lipid becomes the limiting factor [16].

In the present work, static Franz glass diffusion cells have been used in order to evaluate the release profile of clotrimazole from SLN and NLC, in comparison to the release of the same drug from commercial creams. Static Franz glass structure is schematically represented in Fig. 3.12.

These cells consist of donor (1) and acceptor (2) chambers between which a diffusion membrane (3) is positioned [304]. Cellulose nitrate membranes (Sartorius, Germany) with an average pore size of 0.1 µm were used. In the present work, the area for diffusion was 0.64 cm<sup>2</sup> and the acceptor chamber volume was approximately 5.5 ml. A magnetic stirring (4) was placed in the acceptor chamber previously to the assay. The acceptor chamber was maintained

at 32°C using a water bath (5), in order to ensure the surface skin temperature at the surface of the membrane. Samples were collected from the acceptor medium (6) using a micro-syringe.

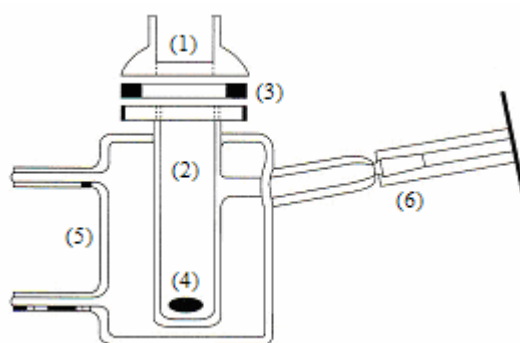


**Fig. 3.12: Schematic representation of a static Franz cell. (1) donor compartment; (2) acceptor compartment; (3) cellulose nitrate membrane; (4) magnetic stirring; (5) thermostated water bath; (6) sampling device.**

The acceptor medium consisted of a solution of 100 mM acetate buffer, pH 6.0 with 35% (v/v) of dioxane. The inclusion of 35% (v/v) of dioxane in the composition of the acceptor medium is due to the insufficient solubility of clotrimazole in the 100 mM acetate buffer solution. Since the acceptor medium was not intended to mimic skin conditions, it was suitable for the present *in vitro* investigations. A volume of 250  $\mu$ l of an aqueous SLN dispersion (containing 1% of drug) or 250 mg of the respective cream was applied to the donor compartment. Samples (250  $\mu$ l) were collected over 24 hr and analysed by spectrophotometric determination at 243 nm in a path length of 1 cm at 20 $\pm$ 1°C. After each sample taking, the Franz cells were filled up with acceptor medium. For each formulation, the release studies were performed in triplicate.

UV spectrophotometric quantifications of clotrimazole were carried out using an Uvikon 940 double-beam spectrophotometer (Kontron Instruments, Eching, Germany). Validation of the method was performed regarding the linearity, precision, accuracy, selectivity, sensitivity and stability. Calibration curves have been obtained from a series of standard solutions of clotrimazole in the acceptor medium ranging from 25 to 150  $\mu$ g/ml. The 100 mM acetate buffer pH 6.0 with 35% (v/v) of dioxane was used as blank. Fig. 3.13 shows the obtained calibration curve.

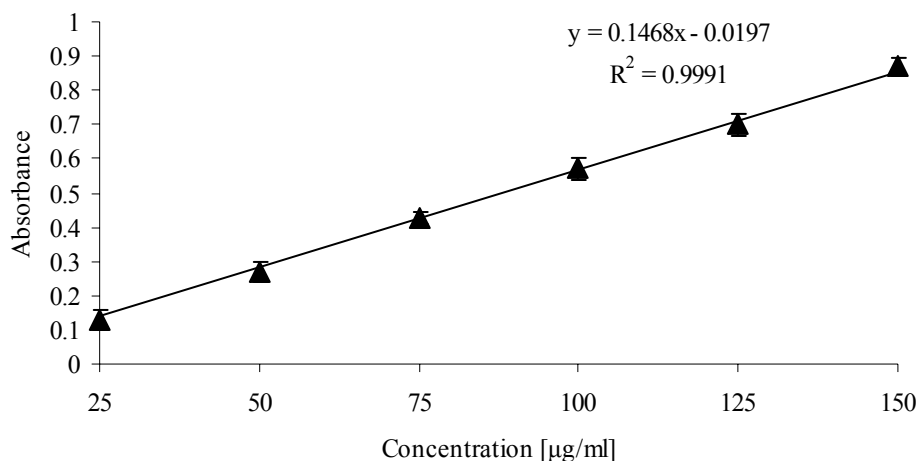


**Fig. 3.13: Calibration curve of clotrimazole in a solution of 100 mM acetate buffer, pH 6.0 with 35% (v/v) of dioxane.**

The amount of released clotrimazole was assessed by measuring the absorbance of the samples directly after their collection from Franz cells. The amount of drug permeating through the cellulose nitrate membrane during a sampling interval was calculated based on the measured reservoir concentration and volume. Plots of amount permeating vs time were made for each experiment. Flux was calculated as the slope of the linear portion of the plot and was normalized to 1 cm<sup>2</sup> surface area. The flux was expressed as the percentage of the applied amount delivered per hr and it was not correlated for the surface area. All flux data are reported as the mean value of at least three determinations.

### 3.2.9 Rheological analysis of developed formulations

Rheological measurements are a valuable tool for quality control of pharmaceutical formulations, intended for topical and dermatological applications, together with manufacturing processes, such as mixing, pumping, stirring, filling and sterilization [218].

Concerning liquid dispersions of lipid nanoparticles, they usually need to be incorporated in convenient topical dosage forms, such as creams, ointments or hydrogels, to obtain a topical application form having the desired semi-solid consistency. However, when incorporated into a semi-solid base, the physicochemical characteristics of SLN and NLC can be modified as a result of interactions between the components of the final product, which can be evaluated using the so-called rheological measurements.

Semi-solid systems are characterized as materials that retain their shape when unconfined, but flow or deform when an external force is applied. Essential components for a rheological

observation are the tangential application of a force to a body and the resultant deformation of that body [305]. If this force is applied for a short period of time and then withdrawn, the deformation is defined as elastic if the shape is restored or flow if the deformation remains. A fluid or liquid becomes a body that flows under the action of an infinitesimal force. In practice, gravity is generally regarded as the criterion of such a minimal force.

Fig. 3.14 represents the model demonstrating the components of the classic viscous flow [305]. Two parallel planes are at a distance  $x$  apart, and between these planes the viscous body is confined. The top plane  $A$  moves horizontally with the velocity  $v$  because of the action of force  $F$ . The lower plane  $B$  is motionless. As a consequence, there exists a velocity gradient between the planes  $dv/dx$ . This gradient is given by the definition of rate of shear  $Gp$ . The shear stress  $\tau$  is the force per unit of area creating the deformation.

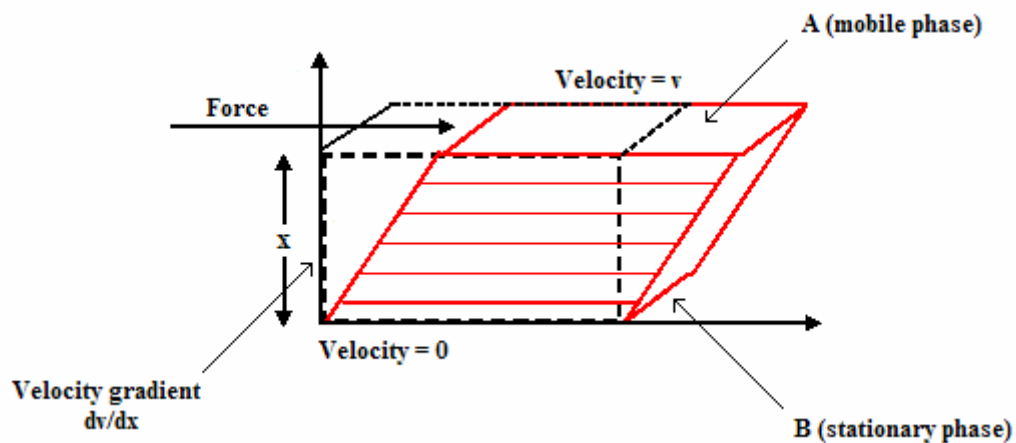


**Fig. 3.14: Schematic model for demonstrating the components of classic viscous flow (modified after Wood [305]).**

The shear stress may be applied either momentarily or continuously. Elastic deformation occurs if, as the force is applied, the upper plate moves in the direction of the force only momentarily and then stops but returns to its original position when the deforming force is removed. On the other hand, pure viscous flow occurs if there is a continuous movement during the applied force, and no restorative motion follows removal of the deforming force.

Between the limits of elastic deformation and pure viscous flow, a continuum of combinations of these limits exists. Such behaviour is called viscoelastic flow. A newtonian fluid is a fluid in which a direct proportionality exists between shear stress and shear rate, for all values of shear.

Viscosity or coefficient of viscosity is the proportionality constant between shear stress  $\tau$  and shear rate  $Gp$ . Conventionally, viscosity is represented by  $\eta$  and it is given by:

$$\eta = \frac{\tau}{Gp} \quad (14)$$

Fluidity is the reciprocal of the viscosity, usually designed by the symbol  $\Phi$ . Kinematic viscosity  $\nu$  is the Newtonian viscosity divided by density  $d$ :

$$\nu = \frac{\eta}{d} \quad (15)$$

Non-newtonian fluids are those for which there is no direct linear relationship between shear stress and shear rate. Most systems of pharmaceutical interest fall into this category. A pseudoplastic material is one in which the stress increases at less than a linear rate with increasing shear rate, while a dilatant material is characterized by a more rapid increase. Thus, if viscosity is calculated at each of a series of shear rate points, by use of the ratio between shear rate and shear stress, then the resultant values decrease with increasing shear rate for pseudoplastic materials and increase for dilatant ones. Measurements at such single points are frequently referred to as apparent viscosity to recognize clearly that the number quoted refers only to the condition of measurement. The fact that one number cannot characterize the viscous behaviour, however, requires the use of some equation of state. One such empiric one is the Power Law Equation:

$$\tau = A[Gp]^n \quad (16)$$

where  $A$  is an appropriate proportionality constant and  $n$  is the Power Index. In equation 16,  $n$  is less than 1 for pseudoplastic materials and greater than 1 for dilatant materials. The Power Law Equation is also used with the index  $n$  associated with shear stress rather than shear rate. When the logarithm of both sides of equation 16 is taken, the result is:

$$\log \tau = \log A + n \log Gp \quad (17)$$

Compared with the equation of a straight line, a plot of  $\log \tau$  against  $\log Gp$  results in a straight line of slope  $n$  and intercept  $\log A$ .

When an initial finite force is necessary before any rheologic flow can start, the initial stress is called yield value  $f$ . A Bingham plastic is represented by a straight line or curve on the stress shear rate plot being displaced from the origin by a finite stress value. Thus, for Newtonian behaviour at stresses greater than the yield value  $f$ , it can be written:

$$\tau - f = U Gp \quad (18)$$

where  $U$  is the plastic viscosity. Similarly, both pseudoplastic and dilatant curves may appear to exhibit yield values. The dimensional units of the yield value must be those of the shear stress.

In general, Newtonian liquids are pure chemicals rather than polymeric materials. All interactions are such that no structure is contributed to the liquid. Once by definition shear stress and shear rate are directly proportional, a single viscometric point can characterize the liquid rheology. Increasing temperature decreases viscosity as it reduces intra-molecular forces of attraction. Such temperature viscosity relationships are quickly established, regardless of whether temperature is increased or decreased.

Pseudoplastic behaviour is exhibited by polymer solutions and by most of the semi-solid systems containing some polymer components.

Thixotropy is a phenomenon resulting from the time dependency of the breakdown or the rebuilding of structure. It is an empiric observation of good reliability that structure breakdown or build-up is an exponential function time. Thus, if the observed shear stress for a given shear rate is followed with time, a plot of stress against time, both on the logarithmic scale, results in a straight line. A coefficient of thixotropic breakdown  $B$  can be calculated by the equation 19:

$$B = \frac{\tau_1 - \tau_2}{\ln(t_2/t_1)} \quad (19)$$

where  $\tau_1$  and  $\tau_2$  are the stress values at times  $t_1$  and  $t_2$  of continuous shear at any arbitrary shear rate chosen for comparison.

Dilatant systems are essentially the opposite of pseudoplastic thixotropic ones. In dilatancy as shear continued, the fluid components contributing to lubricity between the shear planes so that the resulting structure develops increasing friction. Thus, stress increases with time in a logarithmic manner similar to that with thixotropy. A similar hysteresis loop, i.e. a measure of thixotropy in area, of rheopexy is developed in dilatant systems. The equation 19 may be used with dilatant systems in the same way as with thixotropic ones to yield a coefficient of dilatant build-up. To summarise, Fig. 3.15 depicts the four basic types of rheograms or flow curves.

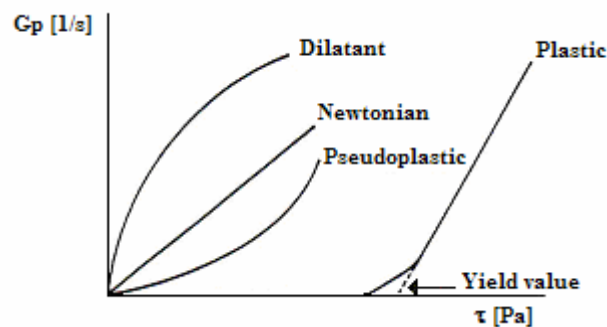


**Fig. 3.15: Schematic representation of the four basic types of rheograms (modified after Barry [218]).**

In the present work, the rheological measurements were performed on a rheometer Rheo Stress RS 100 (Haake Instruments, Karlsruhe, Germany) equipped with a cone-and-plate test geometry (plate diameter 20 mm, cone angle 4°). If not otherwise indicated, all measurements have been carried out at a temperature of 20±0.1°C. Evaluation of the rheological properties of the developed formulations has been performed applying continuous shear investigations and oscillation frequency sweep tests. Continuous shear investigations have been applied to characterize semi-solid formulations, evaluating the shear stress as a function of shear rate. In order to determine if the systems are thixotropic, this study started applying 0 s<sup>-1</sup> up to a maximum shear rate of 100 s<sup>-1</sup> and back to 0 s<sup>-1</sup>, and the resulting shear stress and viscosity were measured.

Oscillation frequency sweep tests have been performed in order to determine the rheological properties of the developed aqueous SLN and NLC dispersions. Oscillation tests are dynamic methods for determining the rheological properties of the material in its rheological ground state without altering its static structure and providing a so-called fingerprint under non-destructive conditions [306, 307].

In an oscillation experiment the material is subject to a sinusoidal stress, providing information on the inter-molecular and inter-particle forces in the material [308]. It can be used to differentiate between two samples which cannot be distinguished by shear experiments, because this test is capable of separating elastic and viscous properties, while shearing leads to an integrated characterization only. The response of the tested material is measured as a function of the frequency at a constant stress amplitude.

The selection of the frequency that is applied has a strong influence on the testing time. The reciprocal of the frequency is the required time to run through one cycle. When applying stress  $\tau$  to a sample, it will deform. Depending on the relationship of viscous and elastic properties, the amplitude of the deformation  $\gamma_0$  is not necessarily reached at the same time as the stress amplitude  $\tau_0$ . There is a phase shift  $\delta$  between stress and deformation.

Pure elastic materials have a phase shift of 0°. For these materials as soon as the force is lowered or released, the deformation recovers. Pure viscous materials have a phase shift of 90° because when the applied force reaches its maximum, the material is pulled apart with its highest speed. Viscoelastic materials show phase shifts between 0 and 90°. For the evaluation of an oscillation experiment the equation 20 is used:

$$\tau_0 = G^* \gamma_0 \quad (20)$$

where  $G^*$  is the complex modulus. By setting the stress amplitude and measuring the deformation amplitude,  $G^*$  can be calculated. By knowing the frequency and measuring the



time at which stress and strain (deformation) amplitudes are reached, the phase shift between both can be calculated, which is then used to determine the storage and the loss moduli. The storage modulus  $G'$  gives information about the elastic component and it can be determined using the equation 21:

$$G' = G^* \cos(\delta) \quad (21)$$

For a purely elastic material the phase shift is  $0^\circ$ , which makes  $\cos(\delta)$  equals to 1, and consequently,  $G'$  is 100%, reflecting the integral character  $G^*$ . The loss modulus  $G''$  is a measure of the viscous component and it can be determined using the equation 22:

$$G'' = G^* \sin(\delta) \quad (22)$$

For a purely viscous material the phase shift is  $90^\circ$ , which makes  $\sin(\delta)$  equals to 1, and consequently,  $G''$  is 100%, reflects the integral character  $G^*$ .

One might be interested in the ratio of viscous and elastic properties, which is given by the equation 23:

$$\frac{G''}{G'} = \frac{\sin(\delta)}{\cos(\delta)} = \tan(\delta) \quad (23)$$

The complex dynamic viscosity  $\eta^*$  is given by the equation 24:

$$\eta^* = \frac{G^*}{\omega} \quad (24)$$

where  $\omega$  is the frequency defined as sinus wave.

Oscillation stress sweep tests have been carried out at a constant frequency of 1 Hz in a stress range of 100 Pa and the oscillation frequency sweep tests were performed over a frequency range from 0 to 10 Hz at constant stress amplitude of 5 Pa for the characterization of Dynasan<sup>®</sup>116-based SLN and NLC, and of 1 Pa for the characterization of Compritol<sup>®</sup>888-based SLN and NLC.

### 3.2.10 Texture analysis of developed formulations

A method that has received recent attention for the characterization of semi-solid pharmaceutical systems is the texture profile analysis [309]. The purpose of the texture analysis of semi-solid formulations is to mathematically characterize the effects of defined experimental parameters, such as probe speed and the ratio of the probe diameter to the diameter of the sample container, on the textural/mechanical properties of the systems under study. The importance of these studies is related to both clinical and non-clinical performance of polymer gels, which are dependent on their mechanical/rheological properties. In addition,

they are applicable to a wide range of sample types, have a short analysis time, little time required for the development of the method, and direct relevance to the sensory properties of topical formulations. However, there are two major disadvantages to be mentioned. First, because of the wide variations in experimental conditions that has been used to characterize other systems and therefore no standard tests have been until now established for SLN- and NLC-based semi-solid formulations. Secondly, is the use of parameters that have no direct rheological significance. This means that it might not be possible to establish some relationship with the recorded rheological data [309].

Several parameters can be measured according to the performance of the sample, i.e. its sensitiveness. For the characterization of the developed semi-solid systems three different parameters have been evaluated, i.e. adhesiveness, consistency and gel strength. Such parameters have been used in the development of pharmaceutical semi-solid systems to provide information related, for example, to the ease of application of the product on the skin or mucosa, and also to the potential bioadhesive properties of the formulations [310, 311]. These mechanical properties have been assessed using the texture analyser TA-XTPlus from Stable Micro Systems, (Goldalming, UK). Data acquisition and mathematical analysis have been performed using a computer equipped with the Texture Expert<sup>®</sup> software.

### **3.2.10.1 Adhesiveness**

Adhesiveness is defined as the work necessary to overcome the attractive forces between the surface of the sample and the surface of the probe with which the sample comes into contact [309]. It is the negative force area and represents the work required to overcome the attractive forces between the surface of the sample and the surface of other materials with which the sample comes into contact, i.e. the total force necessary to pull the compression plunger away from the sample. For materials with high adhesiveness and low cohesiveness, when tested, part of the sample is likely to adhere to the probe on the upward stroke. To some extent the recording of an adhesive force depends on the extent of compression. Lifting of the sample from the base of the testing platform should, if possible, be avoided as the weight of the sample on the probe would become part of the adhesiveness value. In certain cases, gluing of the sample to the base of a disposable platform has been advised but is not applicable for all samples.

The probe (cylindrical DELRIN steel probe of 10 mm diameter) applied a force of 5 g on the surface of the sample at a test speed of 0.5 mm/sec holding it for 10 sec. After this time the

probe was withdrawn at 8 mm/sec. The maximum force required to separate the probe from the sample was recorded as the stickiness. The stringiness value was recorded as the distance the probe was moved away from the sample surface before the force has dropped to 2.5 g. The greater this distance value the more stringy is the product.

This adhesive test has been used to compare the surface stickiness and stringiness of hydrogels loaded with SLN and NLC, as well as to compare their behaviour with pure carbomer gels. For this test the obtained results correspond to the average of three single measurements.

### **3.2.10.2 Consistency**

Consistency is commonly the textural property possessed by pharmaceutical lotions, i.e. fluid products. It most often makes use of the back extrusion rig for its measurements. Sometimes the product may possess particulates. These particulates will affect the repeatability of the results as a different number of particulates will come into contact with the extrusion disk of each test. If the product cannot be tested without the inclusion of particulates then it is recommended to use larger container and larger extrusion disk for assessment. This effectively increases the volume of product tested under the surface and therefore it is used as an averaging effect.

The consistency test was based on the use of a cylindrical DELRIN steel probe of 10 mm diameter, which was applied at a test speed of 2 mm/sec using a force of 2 g. When this surface trigger is attained (i.e. the point at which the disc's lower a surface is in full contact with the sample) the disc proceeds to penetrate to a depth of 2 mm. At this point (most likely to be the maximum force), the probe returns to its original position. The peak of maximum force is taken as a measurement of firmness, i.e. the higher the value the firmer is the sample. For this test the obtained results correspond to the average of three single measurements.

### **3.2.10.3 Gel strength**

Gel strength is measured as the penetration force required for breaking the gels. Concerning the gel strength test, a probe (cylindrical STAINLESS steel probe of 3 mm diameter) was applied by means of a trigger force of 1 g on the surface of the sample at a test speed of 2 mm/sec to a depth of 2 mm. At this depth the maximum force reading is obtained and

translated as the gel strength. For this test the obtained results correspond to the average of three single measurements.

### **3.2.11 Data presentation and statistical treatment in figures and tables**

The data points in figures correspond to the average (mean) value of  $n$  repetitions of the experiment. The error bars stand for the corresponding standard deviations (SD). Data given in tables and in the text are average (mean) values of  $n$  repetitions  $\pm$  SD thereof.